NASA MEMO 1-15-59L

NASA MEMO 1-15-59L

NASA

MEMORANDUM

EFFECTS OF FUSELAGE NOSE LENGTH AND A CANOPY ON THE LOW-SPEED OSCILLATORY YAWING DERIVATIVES OF A SWEPT-WING AIRPLANE MODEL WITH A FUSELAGE OF CIRCULAR CROSS SECTION

By James L. Williams and Joseph R. DiCamillo

Langley Research Center
Langley Field, Va.

NATIONAL AERONAUTICS AND SPACE ADMINISTRATION
WASHINGTON
January 1959

NATIONAL AERONAUTICS AND SPACE ADMINISTRATION

MEMORANDUM 1-15-59L

EFFECTS OF FUSELAGE NOSE LENGTH AND A CANOPY ON THE LOW-SPEED OSCILLATORY YAWING DERIVATIVES OF A SWEPT-WING AIRPLANE MODEL WITH A FUSELAGE OF CIRCULAR CROSS SECTION

By James L. Williams and Joseph R. DiCamillo

SUMMARY

A wind-tunnel investigation was made at low speed in the Langley stability tunnel in order to determine the effects of fuselage nose length and a canopy on the oscillatory yawing derivatives of a complete swept-wing model configuration. The changes in nose length caused the fuselage fineness ratio to vary from 6.67 to 9.18. Data were obtained at various frequencies and amplitudes for angles of attack from 0° to about 32°. Static lateral and longitudinal stability data are also presented.

INTRODUCTION

The results of previous wind-tunnel investigations (refs. 1 to 4) have indicated that wings of swept design have lateral oscillatory stability derivatives that become increasingly large at high angles of attack. These results also showed that the oscillatory derivatives are, in some cases, substantially different from the steady-state derivatives. Some results of reference 3 have shown that the large magnitude of the derivatives at high angles of attack is dependent to some degree on frequency and amplitude of the oscillatory motion. There are certain airplane parameters, also, which may have a modifying effect on the magnitude of these oscillatory derivatives. For fuselages with square cross section, for instance, the fuselage nose length and the canopy have considerable effect on certain static stability derivatives. (See ref. 5.) No data on the dynamic derivatives were given in reference 5, however.

In the present investigation the oscillatory technique of reference 3 was employed for the purpose of determining the effects of fuselage nose length and a canopy on the oscillatory lateral stability derivatives of a complete swept-wing model with circular fuselage cross section at various frequencies and amplitudes.

COEFFICIENTS AND SYMBOLS

The data are presented in the form of coefficients of forces and moments which are referred to the system of stability axes with the origin at the projection on the plane of symmetry of the quarter-chord point of the mean aerodynamic chord. The positive directions of forces, moments, and angular displacements are shown in figure 1. The coefficients and symbols used are defined as follows:

b wing span, ft

C_D' approximate drag coefficient, $\frac{\text{Approximate drag}}{qS}$

C_L lift coefficient, $\frac{\text{Lift}}{qS}$

C_l rolling-moment coefficient, $\frac{\text{Rolling moment}}{qSb}$

C_m pitching-moment coefficient, $\frac{\text{Pitching moment}}{qS\bar{c}}$

C_n yawing-moment coefficient, $\frac{\text{Yawing moment}}{qSb}$

c wing chord, ft

$\bar{c}$ wing mean aerodynamic chord, ft

k reduced frequency parameter, $\omega b/2V$

q dynamic pressure, $\frac{1}{2}\rho V^2$, lb/sq ft

r angular velocity in yaw $(r = \dot{\psi})$, radians/sec

$\dot{r} = \frac{\partial r}{\partial t}$, radians/sec^2

S	wing area, sq ft
t	time, sec
V	free-stream velocity, ft/sec
α	angle of attack, deg
β	angle of sideslip, radians or deg

$\dot{\beta} = \frac{\partial\beta}{\partial t}$, radians/sec

ρ	mass density of air, slugs/cu ft
ψ	angle of yaw, radians or deg
ψ_o	amplitude of yawing oscillation, deg
ω	circular frequency of oscillation, radians/sec

$$C_{l_r} = \frac{\partial C_l}{\partial \frac{rb}{2V}} \qquad C_{n_r} = \frac{\partial C_n}{\partial \frac{rb}{2V}}$$

$$C_{l_{\dot{r}}} = \frac{\partial C_l}{\partial \frac{\dot{r}b^2}{4V^2}} \qquad C_{n_{\dot{r}}} = \frac{\partial C_n}{\partial \frac{\dot{r}b^2}{4V^2}}$$

$$C_{l_\beta} = \frac{\partial C_l}{\partial \beta} \qquad C_{n_\beta} = \frac{\partial C_n}{\partial \beta}$$

$$C_{l_{\dot{\beta}}} = \frac{\partial C_l}{\partial \frac{\dot{\beta}b}{2V}} \qquad C_{n_{\dot{\beta}}} = \frac{\partial C_n}{\partial \frac{\dot{\beta}b}{2V}}$$

Subscript:

40, 45, 50, 55 overall fuselage length, in.

The subscript ω when used with a derivative $\left(\text{for example, } C_{l_{\beta,\omega}} + k^2 C_{l_{\dot{r},\omega}}\right)$ indicates that the derivative was obtained from an oscillation test.

Model designations:

F	fuselage
W	wing
VH	vertical and horizontal tails
WF	wing and fuselage

APPARATUS

The apparatus used in the present investigation for the oscillation-in-yaw tests is described in detail in reference 3. The oscillatory rolling and yawing moments were measured by a two-component resistance-type strain gage attached at the assumed center-of-gravity location of the models. The output signals from the strain gage were modified by a sine-cosine resolver so that the measured signals were proportional to the in-phase and out-of-phase components of the strain-gage signals. These signals were read on a highly damped direct-current meter. This recording equipment is described in detail in the appendix of reference 1.

MODELS

Drawings of the models used in the present investigation are presented as figure 2, and a photograph of a model is presented as figure 3. Pertinent geometric details are given in table I. In order to maintain about the same amount of directional stability for each model at $\alpha = 0^{\circ}$, a different size vertical tail (with aspect ratio of 1.4) was used with each fuselage. All model components (wing, fuselage, and tails) were made of balsa wood with a fiber-glass covering. The wing and tail surfaces had a 45° sweptback quarter-chord line, a taper ratio of 0.6, and NACA 65A008 airfoil sections parallel to the airstream. The wing and horizontal tail, which were common to all models, had aspect ratios of 3 and 4, respectively, and each was mounted in a low position on the fuselage. The fuselages were of circular cross section with a pointed nose and blunt trailing edge. The fuselage fineness ratio varied from 6.67 to 9.18. (Fuselage length varied from 40 inches to 55 inches.) Fuselage coordinates are given in table II. The canopy dimensions selected were average values determined from several present-day fighter-type airplanes. The canopy was located at the same distance from the nose of each fuselage, and thus its distance from the tail assembly varied with the length of the fuselage nose. (See fig. 2(b).) Canopy coordinates are given in table III.

TESTS

All tests were made in the 6- by 6-foot test section of the Langley stability tunnel (ref. 6) at a dynamic pressure of 24.9 pounds per square foot, which corresponds to a Mach number of 0.13. The test Reynolds number based on the mean aerodynamic chord was approximately 0.83×10^6. The oscillation tests consisted of measurements of the in-phase and out-of-phase rolling and yawing moments for a range of frequencies and amplitudes. The $WF_{50}VH$ configuration was oscillated at frequencies of 0.5, 1.0, 1.5, and 2.0 cycles per second at amplitudes of yawing oscillation of $\pm 2^{\circ}$, $\pm 6^{\circ}$, $\pm 10^{\circ}$. These frequencies correspond to values of the reduced-frequency parameter $\omega b/2V$ of 0.0282, 0.0564, 0.0846, and 0.1129. Breakdown tests were made only with the $WF_{50}VH$ configuration at 1.5 cycles per second and an amplitude of yawing oscillation of $\pm 6^{\circ}$. The effect of a canopy on the complete model configurations for the various fuselage lengths was also determined only at a frequency of 1.5 cycles per second and an amplitude of yawing oscillation of $\pm 6^{\circ}$.

For each amplitude, frequency, and angle-of-attack condition, a wind-on and a wind-off test was made. The effects of the inertia of the model were eliminated from the data by subtracting the wind-off results from the wind-on results.

The static derivatives C_{l_β} and C_{n_β} were obtained from tests at $\beta = 0^{\circ}$ and $\beta = \pm 5^{\circ}$ with the same equipment that was used for the oscillation tests. The lift, drag, and pitching-moment results were measured (at $\beta = 0^{\circ}$) by means of a six-component mechanical balance system.

For all tests, oscillatory and static, the angle of attack ranged from 0° to about 32°.

CORRECTIONS

Approximate jet-boundary corrections as determined by the method of reference 7 were applied to the angle of attack and the drag coefficient. For the configurations with horizontal tail, the pitching moment was corrected for the effects of jet boundary by the methods of reference 8. No jet-boundary corrections were applied to the oscillatory results.

The data are not corrected for the effects of blockage and support-strut interference.

RESULTS

The results of the investigation are presented in the following figures:

Figure	Coefficients plotted against α	ψ_o, deg	$\frac{\omega b}{2V}$	Configurations	Canopy
4	$C_{n_{r,\omega}} - C_{n_{\dot{\beta},\omega}}$ $C_{n_{\beta,\omega}} + k^2C_{n_{\dot{r},\omega}}$ $C_{l_{r,\omega}} - C_{l_{\dot{\beta},\omega}}$ $C_{l_{\beta,\omega}} + k^2C_{l_{\dot{r},\omega}}$	±6	0.0846	$WF_{40}VH$ $WF_{45}VH$ $WF_{50}VH$ $WF_{55}VH$	On and off
5	$C_{n_{r,\omega}} - C_{n_{\dot{\beta},\omega}}$ $C_{n_{\beta,\omega}} + k^2C_{n_{\dot{r},\omega}}$ $C_{l_{r,\omega}} - C_{l_{\dot{\beta},\omega}}$ $C_{l_{\beta,\omega}} + k^2C_{l_{\dot{r},\omega}}$	±2, ±6, ±10	0.0282 .0564 .0846 .1129	$WF_{50}VH$	Off
6	$C_{n_{r,\omega}} - C_{n_{\dot{\beta},\omega}}$ $C_{n_{\beta,\omega}} + k^2C_{n_{\dot{r},\omega}}$ $C_{l_{r,\omega}} - C_{l_{\dot{\beta},\omega}}$ $C_{l_{\beta,\omega}} + k^2C_{l_{\dot{r},\omega}}$	±2, ±6, ±10	0.0282 .0564 .0846 .1129	$WF_{50}VH$	Off
7	$C_{n_{\beta}}$, $C_{l_{\beta}}$	0	0	$WF_{40}VH$ $WF_{45}VH$ $WF_{50}VH$ $WF_{55}VH$	On and off
8	$C_{n_{r,\omega}} - C_{n_{\dot{\beta},\omega}}$ $C_{n_{\beta,\omega}} + k^2C_{n_{\dot{r},\omega}}$ $C_{l_{r,\omega}} - C_{l_{\dot{\beta},\omega}}$ $C_{l_{\beta,\omega}} + k^2C_{l_{\dot{r},\omega}}$	±6	0.0846	WF_{50} $F_{50}VH$ $WF_{50}VH$	Off
9	C_m, C_L, C_D'	0	0	$WF_{40}VH$ $WF_{45}VH$ $WF_{50}VH$ $WF_{55}VH$	On and off

Increasing the fuselage nose length by as much as 75 percent and making compensating increases in tail size did not have an undesirable influence on the variation of yaw damping and directional stability with angle of attack. Substantial influences of canopy addition were apparent, however (fig. 4(a)). The effects of changes in frequency and amplitude of motion were also significant. Such effects have been noted in reference 3 for wings alone, but not to such an extent at the lower angles of attack as is shown in the present results for changes in amplitude (fig. 6(a)).

Langley Research Center,
National Aeronautics and Space Administration,
Langley Field, Va., October 1, 1958.

REFERENCES

1. Queijo, M. J., Fletcher, Herman S., Marple, C. G., and Hughes, F. M.: Preliminary Measurements of the Aerodynamic Yawing Derivatives of a Triangular, a Swept, and an Unswept Wing Performing Pure Yawing Oscillations, With a Description of the Instrumentation Employed. NACA RM L55L14, 1956.

2. Campbell, John P., Johnson, Joseph L., Jr., and Hewes, Donald E.: Low-Speed Study of the Effect of Frequency on the Stability Derivatives of Wings Oscillating in Yaw With Particular Reference to High Angle-of-Attack Conditions. NACA RM L55H05, 1955.

3. Fisher, Lewis R.: Experimental Determination of the Effects of Frequency and Amplitude on the Lateral Stability Derivatives for a Delta, a Swept, and an Unswept Wing Oscillating in Yaw. NACA Rep. 1357, 1958. (Supersedes NACA RM L56A19.)

4. Riley, Donald R., Bird, J. D., and Fisher, Lewis R.: Experimental Determination of the Aerodynamic Derivatives Arising From Acceleration in Sideslip for a Triangular, a Swept, and an Unswept Wing. NACA RM L55A07, 1955.

5. Jaquet, Byron M., and Fletcher, H. S.: Effects of Fuselage Nose Length and a Canopy on the Static Longitudinal and Lateral Stability Characteristics of 45° Sweptback Airplane Models Having Fuselages With Square Cross Sections. NACA TN 3961, 1957.

6. Bird, John D., Jaquet, Byron M., and Cowan, John W.: Effect of Fuselage and Tail Surfaces on Low-Speed Yawing Characteristics of a Swept-Wing Model As Determined in Curved-Flow Test Section of Langley Stability Tunnel. NACA TN 2483, 1951. (Supersedes NACA RM L8G13.)

7. Silverstein, Abe, and White, James A.: Wind-Tunnel Interference With Particular Reference to Off-Center Positions of the Wing and to the Downwash at the Tail. NACA Rep. 547, 1936.

8. Gillis, Clarence L., Polhamus, Edward C., and Gray, Joseph L., Jr.: Charts for Determining Jet-Boundary Corrections for Complete Models in the 7- by 10-Foot Closed Rectangular Wind Tunnels. NACA WR L-123, 1945. (Formerly NACA ARR L5G31.)

TABLE I.- PERTINENT GEOMETRIC DETAILS OF MODELS

	F_{40}	F_{45}	F_{50}	F_{55}
Fuselage:				
Length, in.	40	45	50	55
Ratio of length forward of center of gravity to length rearward of center of gravity	1.051	1.308	1.563	1.820
Maximum diameter, in.	6	6	6	6
Fineness ratio	6.67	7.50	8.34	9.18
Side area, sq in.	176.08	206.08	236.08	226.08
Volume, cu in.	681.6	823.0	964.4	1105.8
Maximum cross-sectional area, sq in.	28.26	28.26	28.26	28.26
Vertical tail:				
Total area to fuselage center line, sq in.	48.6	59.0	68.7	79.1
Exposed area, sq in.	35.8	44.8	53.1	62.5
Span from fuselage center line, in.	8.25	9.09	9.81	10.52
Root chord, in.	7.37	8.11	8.76	9.40
Mean aerodynamic chord, in.	6.03	6.64	7.17	7.69
Sweepback of quarter-chord line, deg	45	45	45	45
Taper ratio	0.6	0.6	0.6	0.6
Aspect ratio	1.4	1.4	1.4	1.4
NACA airfoil section parallel to root chord	65A008	65A008	65A008	65A008
Canopy:				
Length, in.	14.00			
Side area, sq in.	11.9			
Maximum cross-sectional area, sq in.	2.40			
Volume, cu in.	17.16			
Ratio of length to maximum width	5.385			
Ratio of distance from fuselage nose to maximum fuselage width	1.00			
Wing:				
Area, sq in.	324.0			
Span, in.	31.18			
Root chord, in.	12.99			
Mean aerodynamic chord, in.	10.63			
Sweepback of quarter-chord line, deg	45			
Taper ratio	0.6			
Aspect ratio	3			
Horizontal tail:				
Total area, sq in.	64.8			
Span, in.	16.10			
Mean aerodynamic chord, in.	5.03			
Sweep of quarter-chord line, deg	45			
Taper ratio	0.6			
Aspect ratio	4			
NACA airfoil section parallel to the plane of symmetry	65A008			

TABLE II.- FUSELAGE COORDINATES

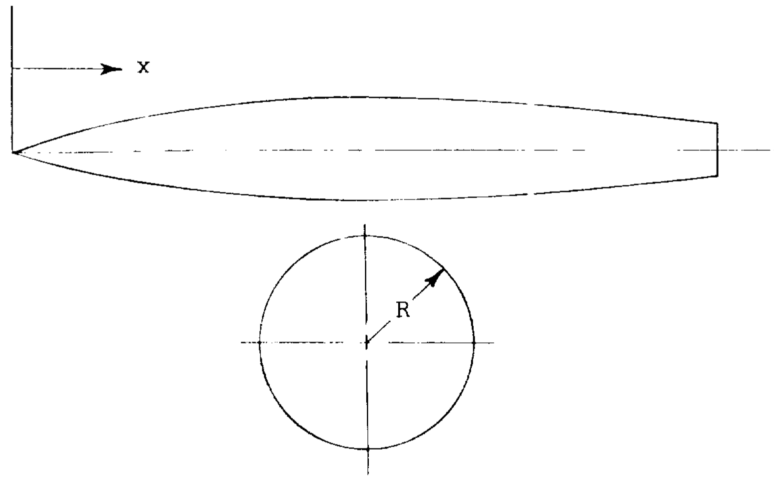

x, in.	R_{40}, in.	R_{45}, in.	R_{50}, in.	R_{55}, in.
0	0	0	0	0
2	.64	.64	.64	.64
4	1.20	1.20	1.20	1.20
6	1.68	1.68	1.68	1.68
8	2.09	2.09	2.09	2.09
10	2.42	2.42	2.42	2.42
12	2.67	2.67	2.67	2.67
14	2.85	2.85	2.85	2.85
16	2.96	2.96	2.96	2.96
18	3.00	3.00	3.00	3.00
20	2.97	2.99	3.00	3.00
22	2.90	2.97	3.00	3.00
24	2.80	2.93	3.00	3.00
26	2.68	2.87	2.99	3.00
28	2.55	2.79	2.95	3.00
30	2.40	2.70	2.90	2.99
32	2.26	2.60	2.83	2.97
34	2.10	2.47	2.75	2.93
36	1.92	2.33	2.65	2.87
38	1.72	2.18	2.54	2.79
40	1.50	2.01	2.40	2.70
42	----	1.82	2.26	2.60
44	----	1.61	2.10	2.47
45	----	1.50	----	----
46	----	----	1.92	2.33
48	----	----	1.72	2.18
50	----	----	1.50	2.01
52	----	----	----	1.82
54	----	----	----	1.61
55	----	----	----	1.50

TABLE III.- CANOPY COORDINATES

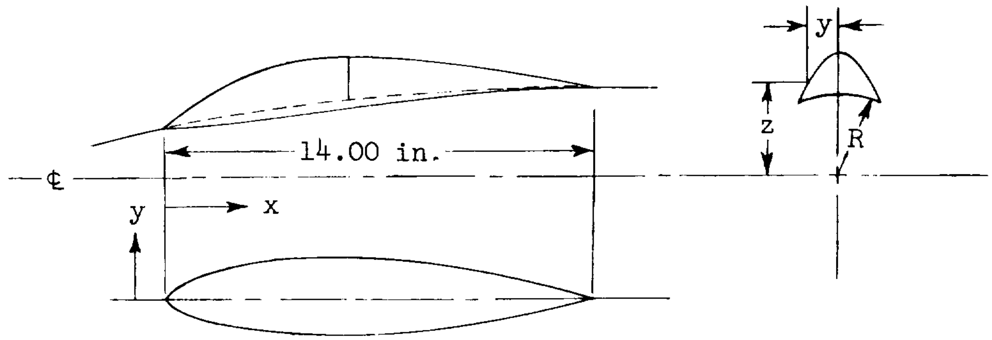

x, in.	y, in.	z, in.	R, in.
0	0	1.68	1.68
1	0.70	1.75	1.89
	.64	1.90	
	.55	2.05	
	.44	2.20	
	.29	2.35	
	0	2.47	
2	0.97	1.85	2.09
	0	3.13	
3	1.16	1.98	2.28
	1.04	2.25	
	.93	2.50	
	.80	2.75	
	.66	3.00	
	.51	3.25	
	.27	3.50	
	0	3.60	
4	1.28	2.06	2.42
	0	3.84	
5	1.30	2.18	2.55
	0	4.00	
6	1.30	2.35	2.67
	1.20	2.60	
	1.07	2.85	
	.95	3.10	
	.81	3.35	
	.67	3.60	
	.46	3.85	
	0	4.09	
7	1.23	2.49	2.77
	0	4.00	
8	1.12	2.63	2.85
	0	3.91	
9	0.95	2.75	2.90
	.84	3.00	
	.68	3.25	
	.50	3.50	
	.22	3.75	
	0	3.80	
10	0.78	2.85	2.96
	0	3.64	
11	0.59	2.93	2.99
	0	3.50	
12	0.40	2.98	3.00
	.34	3.06	
	.25	3.16	
	.14	3.26	
	0	3.36	
13	0.19	2.99	3.00
14	0	3.00	3.00

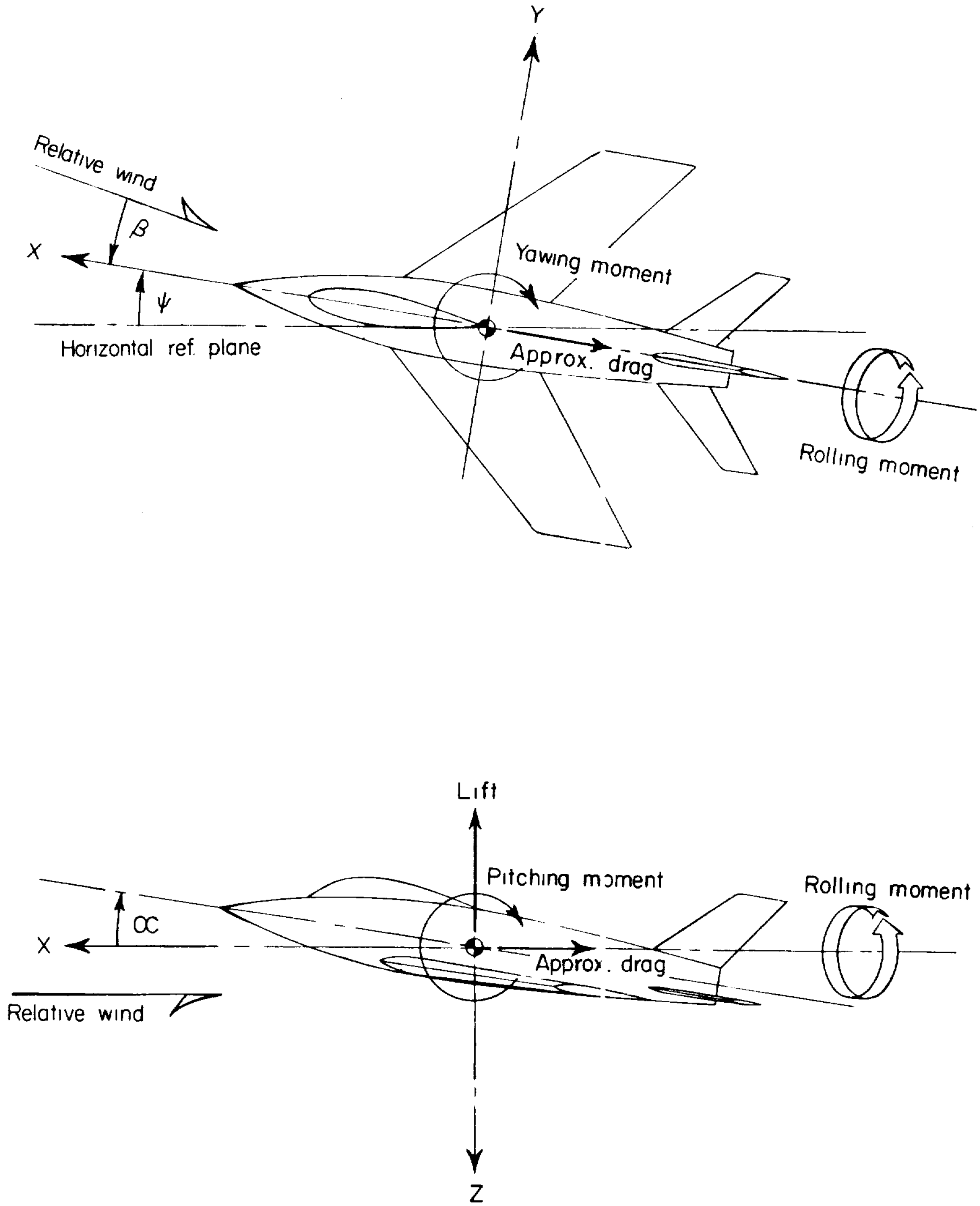

Figure 1.- System of stability axes. Arrows indicate positive directions of forces, moments, and angular displacements.

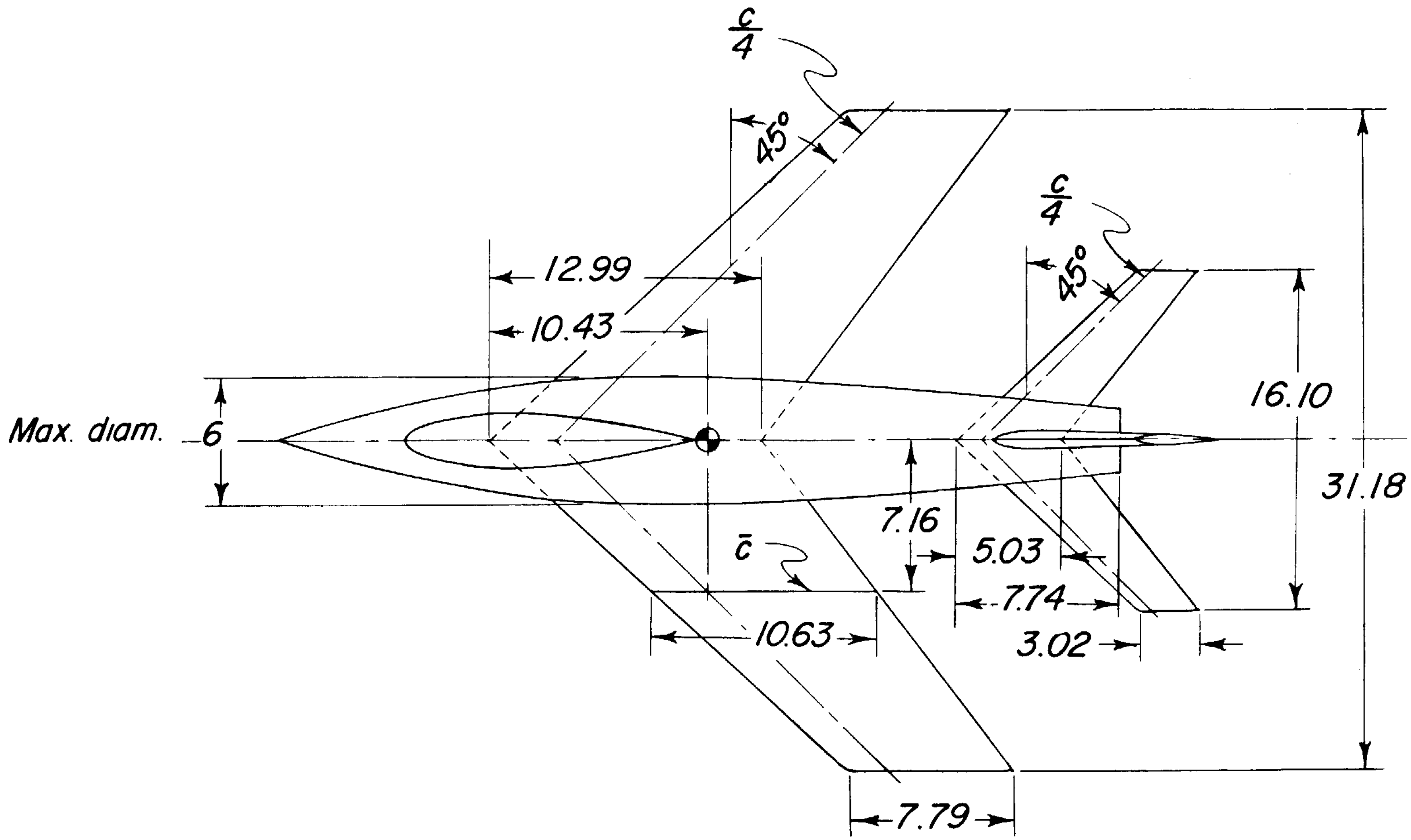

(a) Details of wing and horizontal tail.

Figure 2.- General model arrangement. All dimensions are in inches.

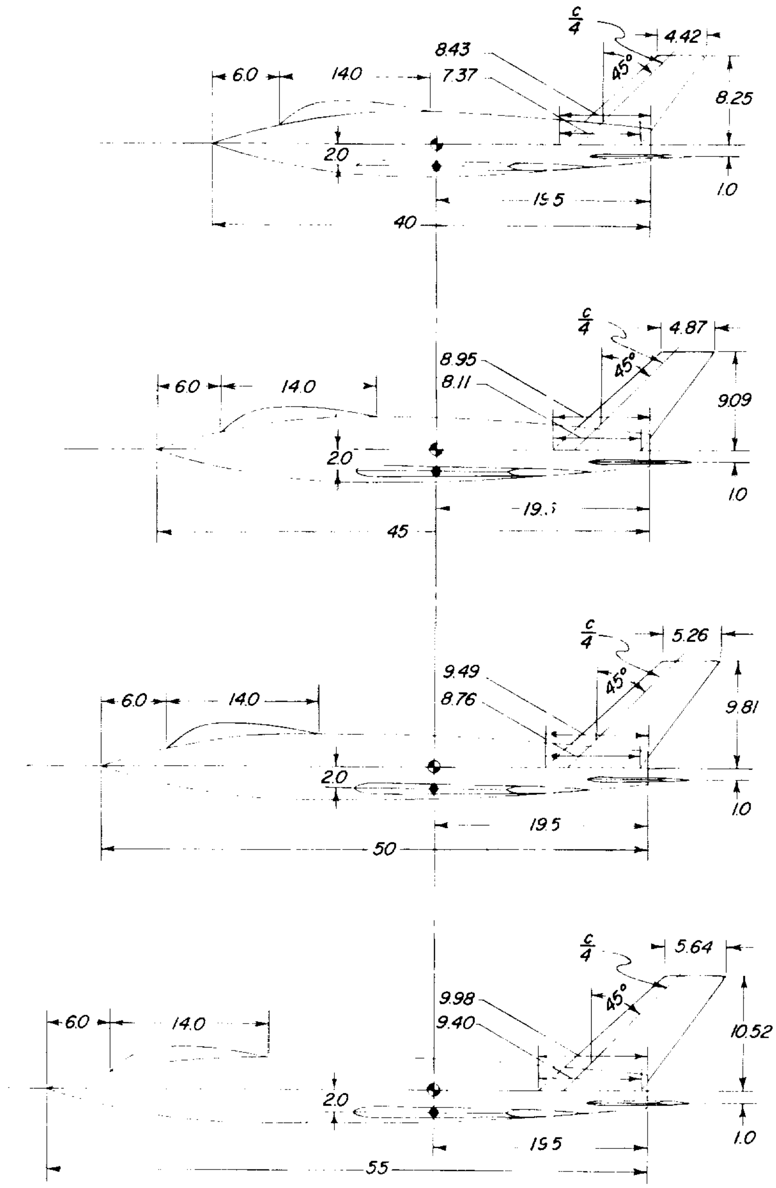

(b) Details of fuselages and vertical tails.

Figure 2.- Concluded.

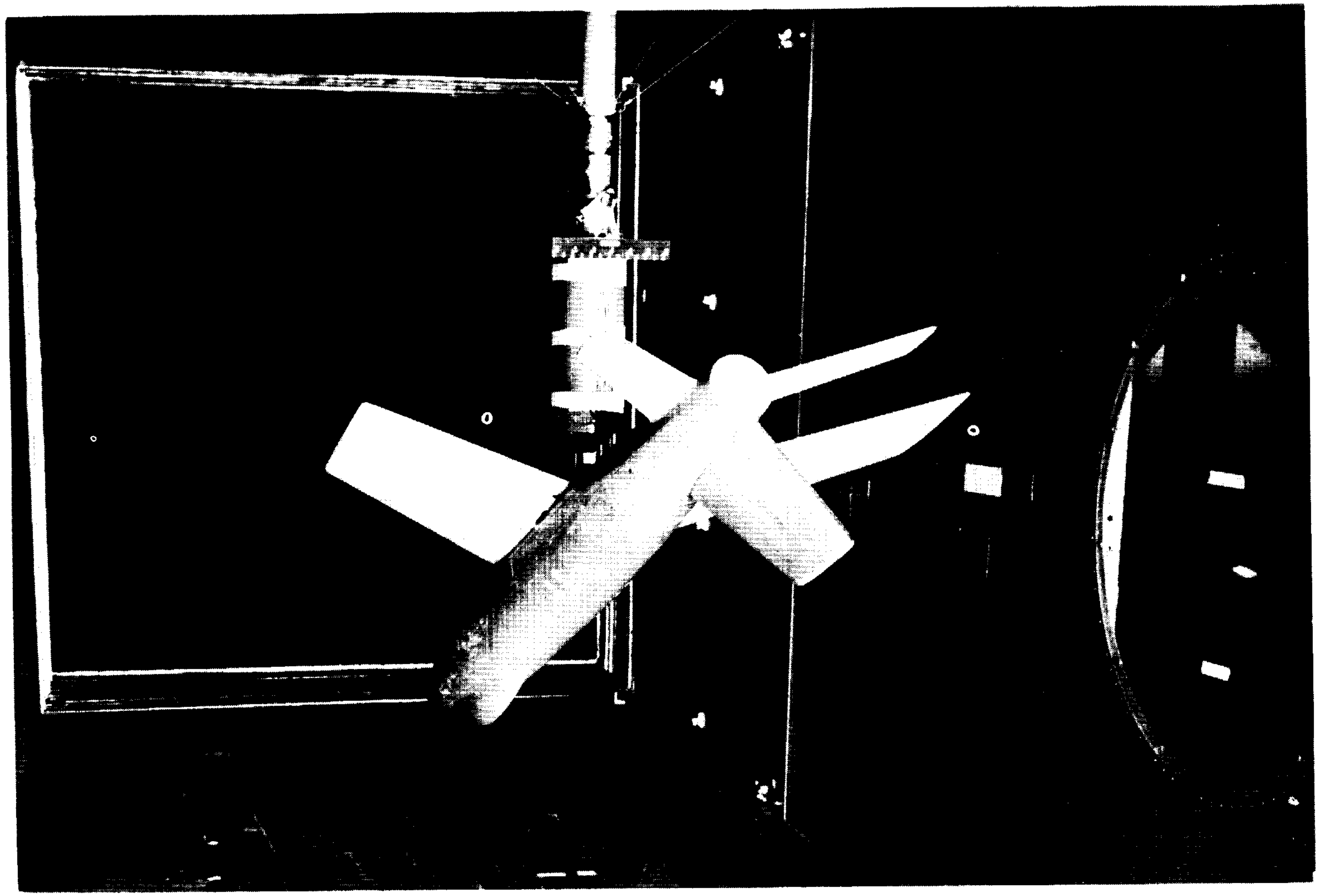

Figure 3.- Photograph of model in tunnel test section. L-57-242

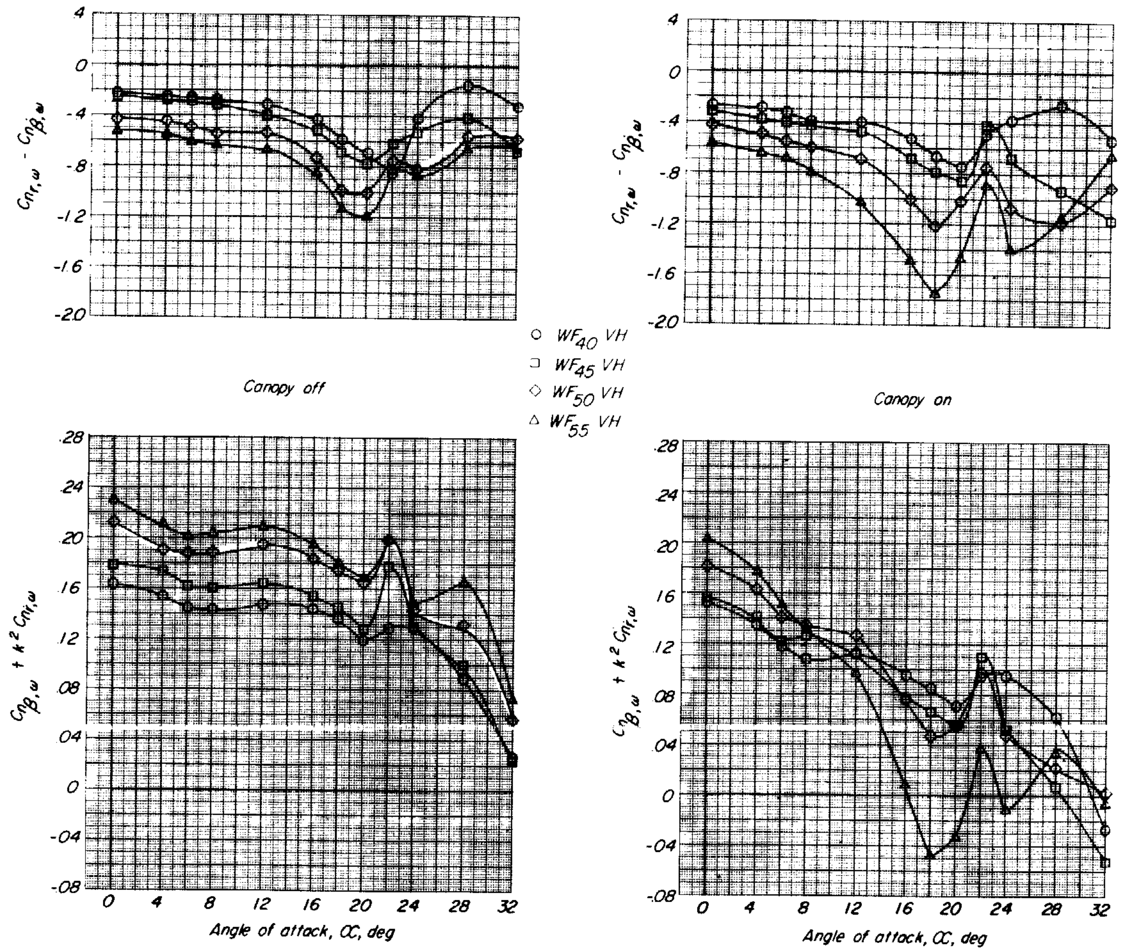

(a) Directional characteristics.

Figure 4.- Effect of fuselage nose length on stability derivatives measured during oscillation for configurations with canopy on and off. $\frac{\omega b}{2V} = 0.0846$; $\psi_o = \pm 6^{\circ}$.

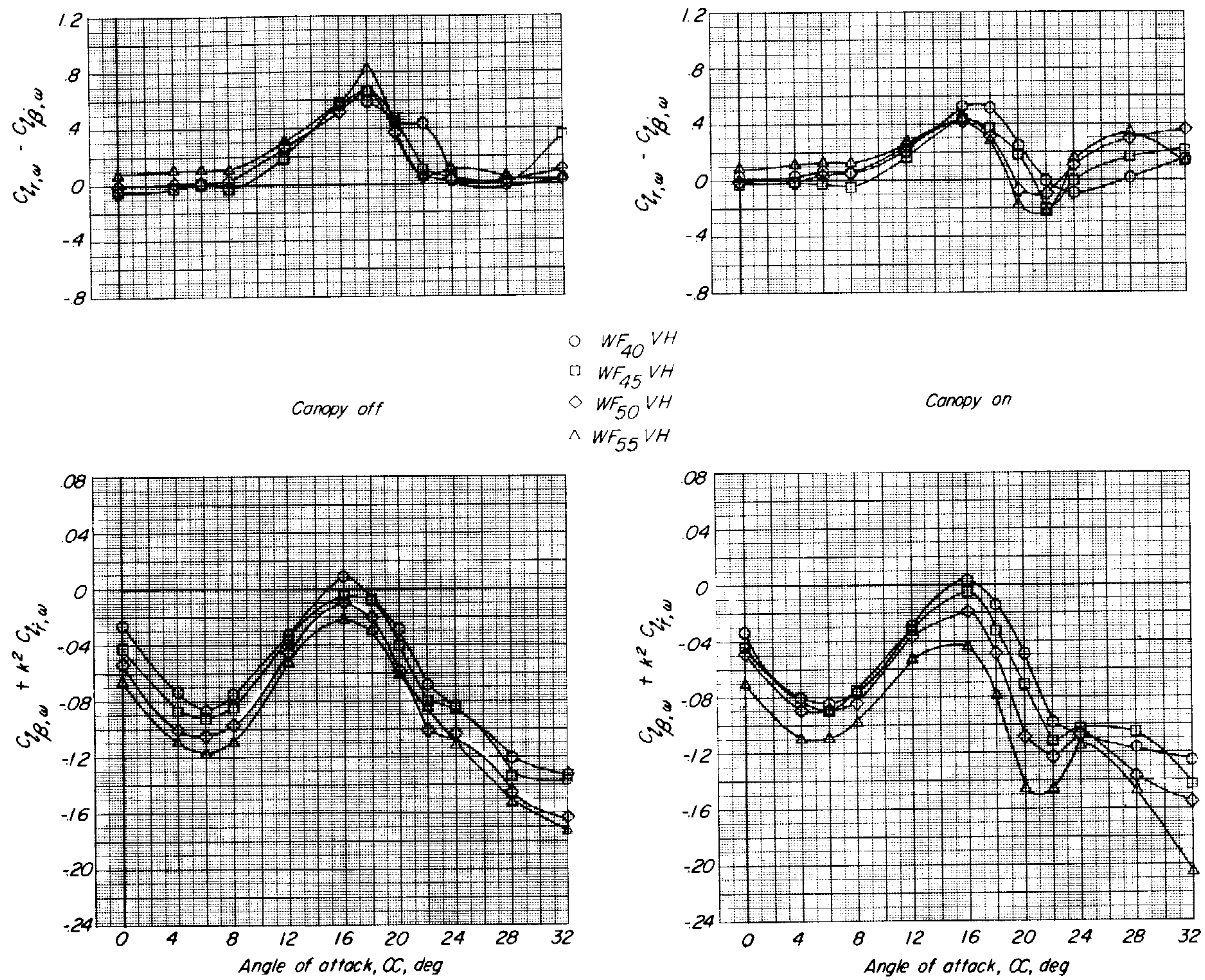

(b) Rolling-moment characteristics.

Figure 4.- Concluded.

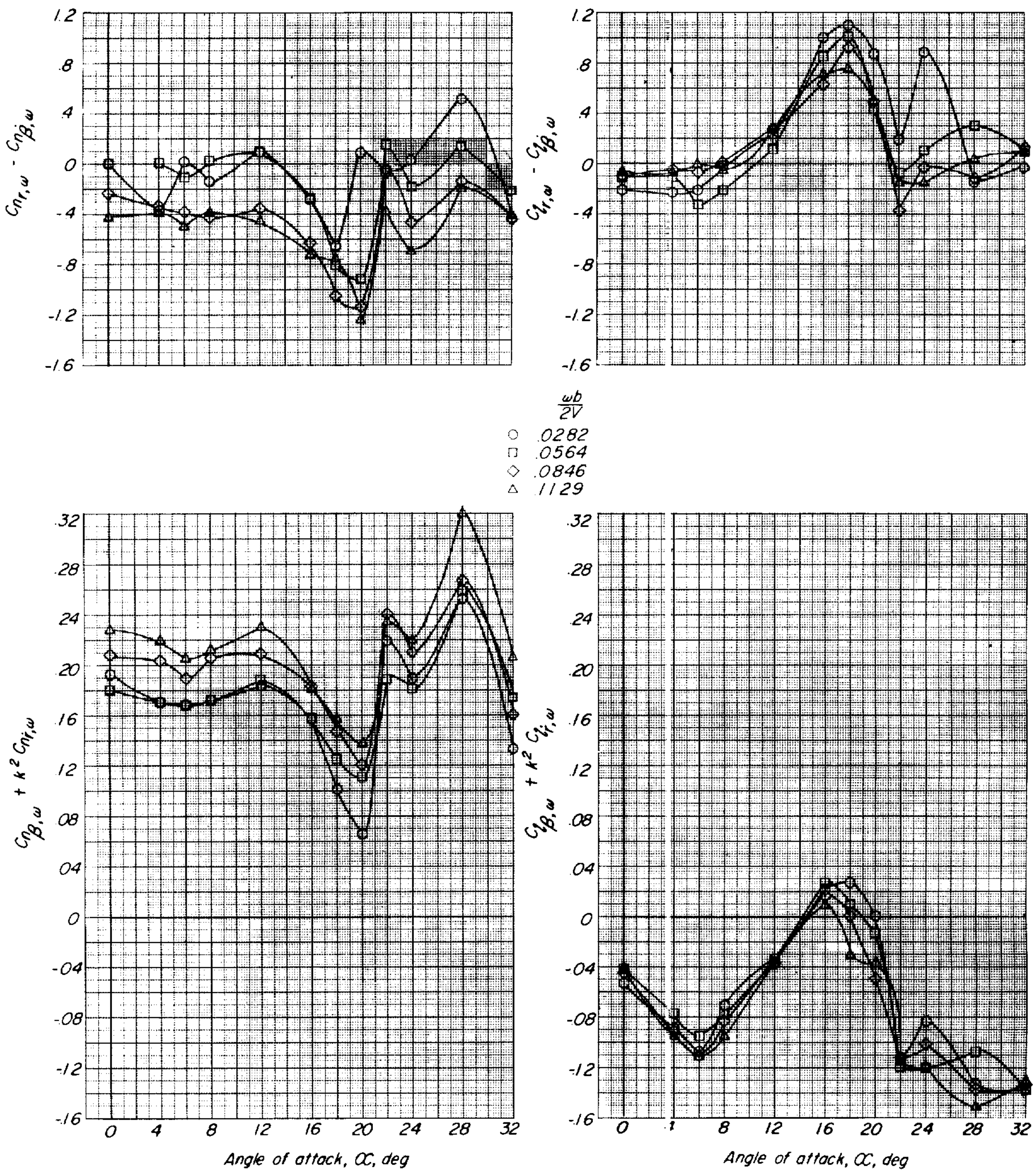

(a) $\psi_o = \pm 2^{\circ}$.

Figure 5.- Effect of reduced frequency parameter on stability derivatives for configuration $WF_{50}VH$ without canopy.

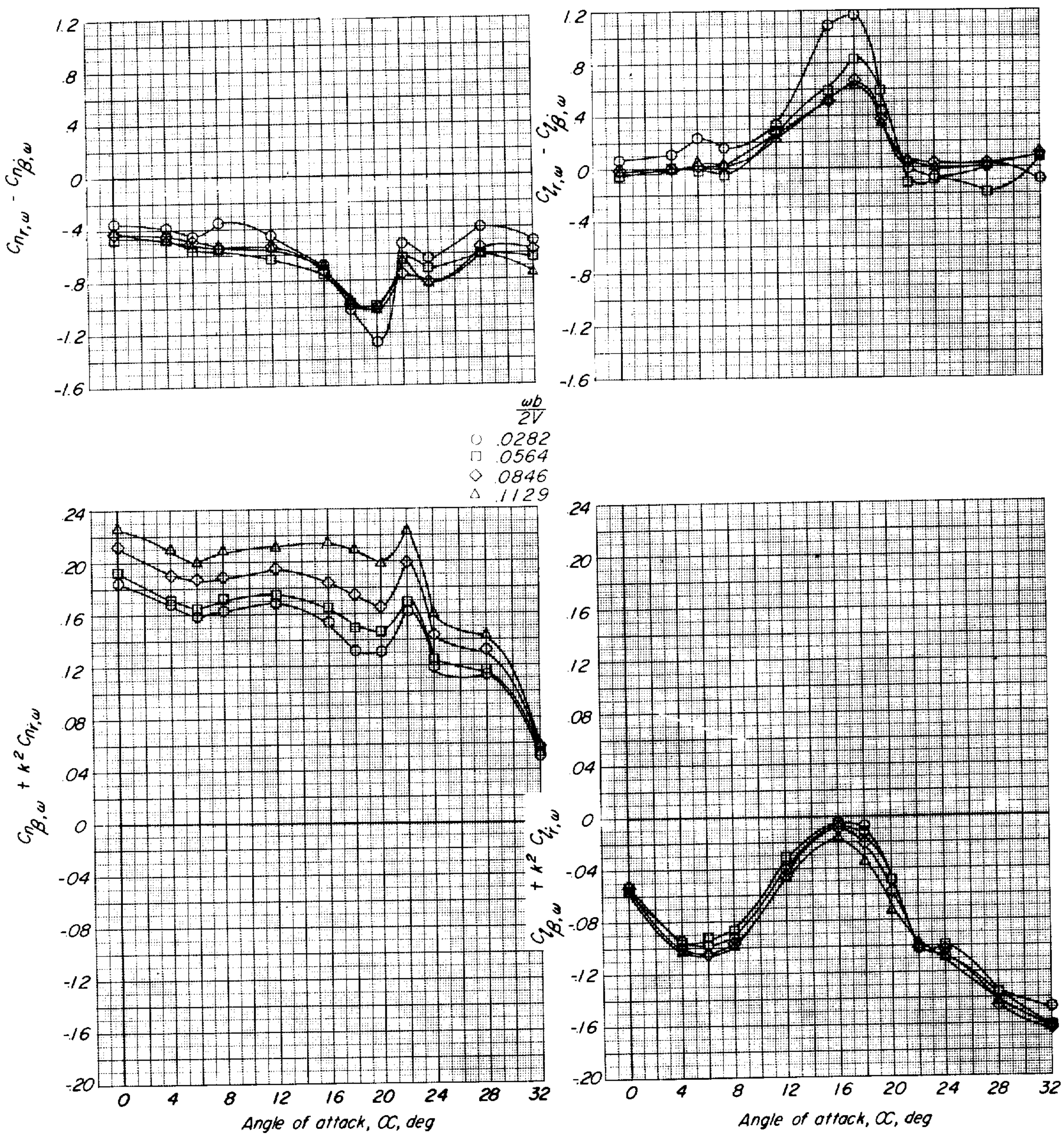

(b) $\psi_o = \pm 6^\circ$.

Figure 5.- Continued.

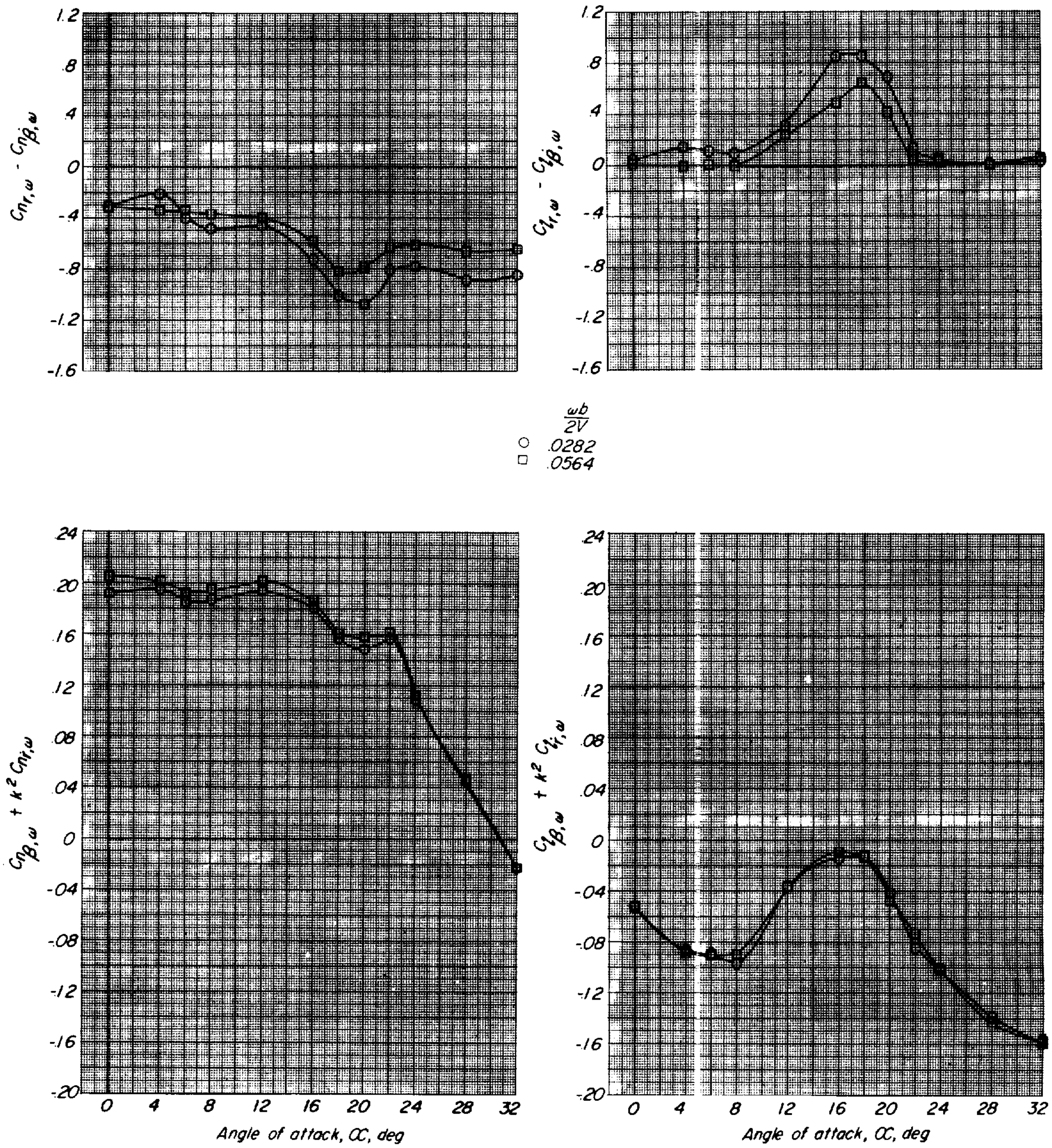

(c) $\psi_o = \pm 10^{\circ}$.

Figure 5.- Concluded.

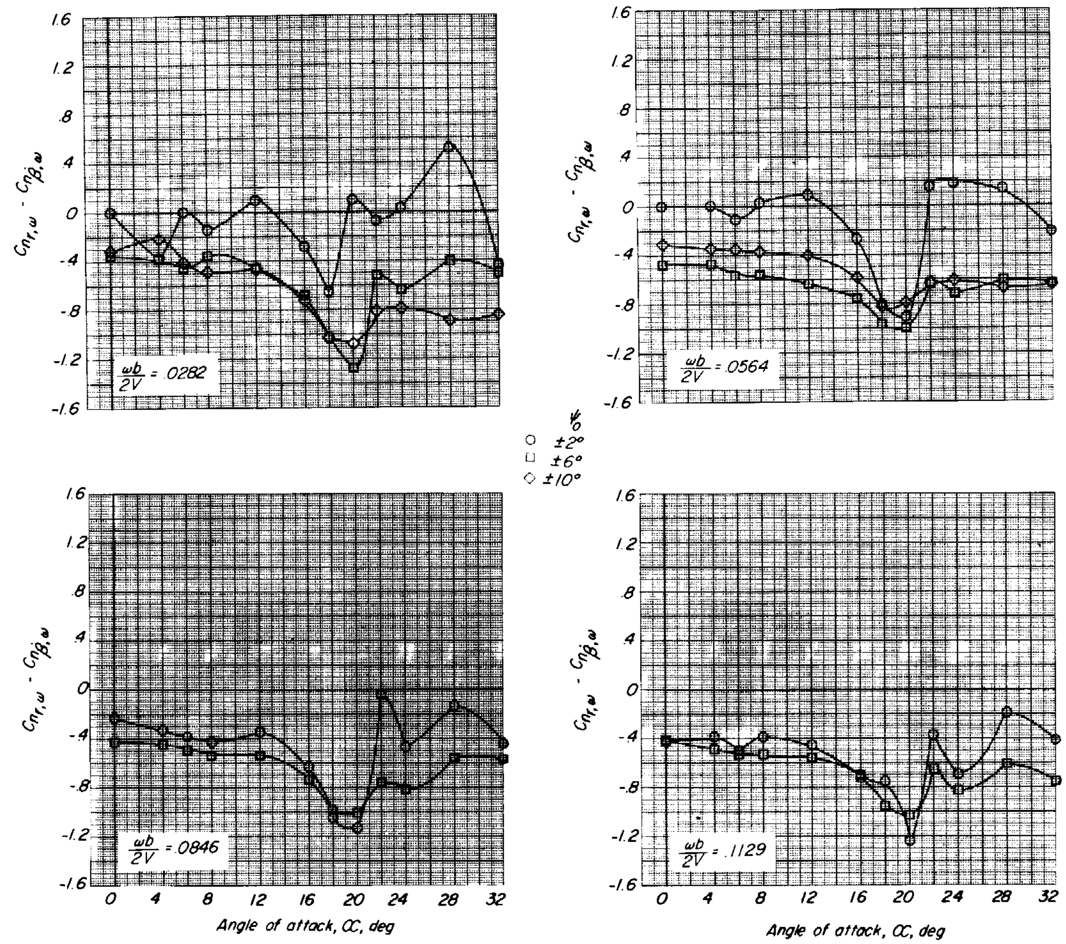

(a) Damping-in-yaw characteristics.

Figure 6.- Effect of amplitude of yaw on oscillatory stability derivatives of configuration $WF_{50}VH$ without canopy.

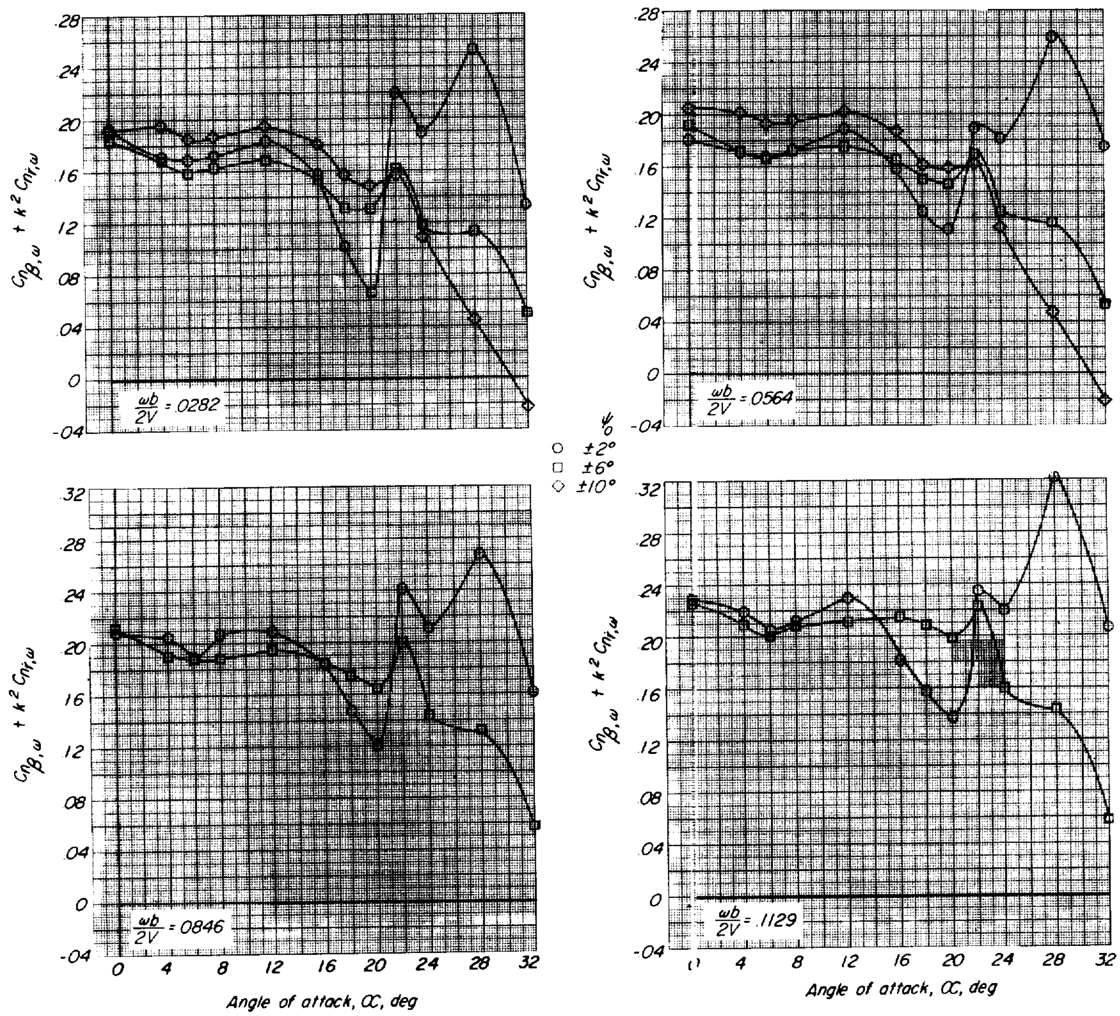

(b) Directional-stability characteristics.

Figure 6.- Continued.

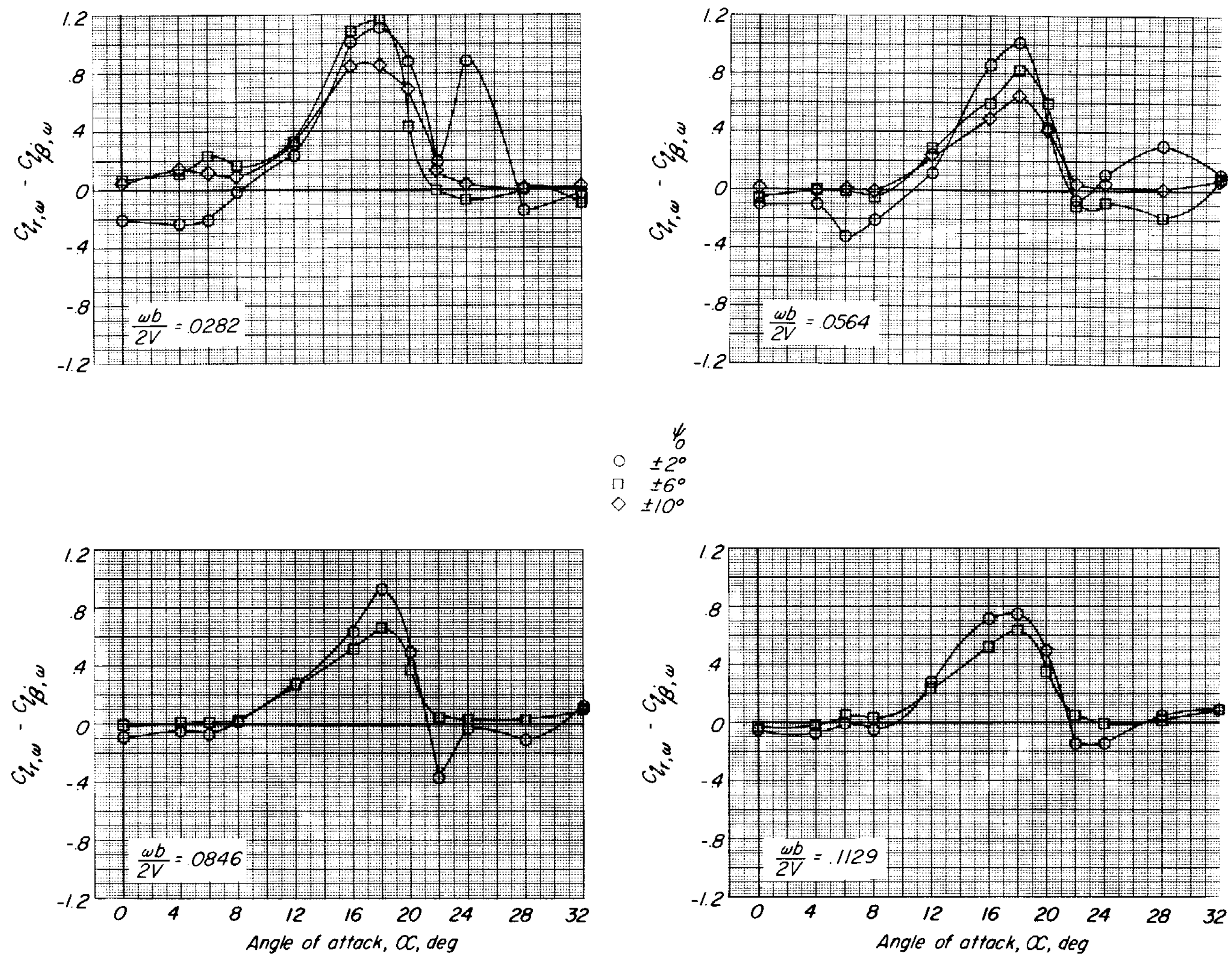

(c) Rolling-moment-due-to-yawing characteristics.

Figure 6.- Continued.

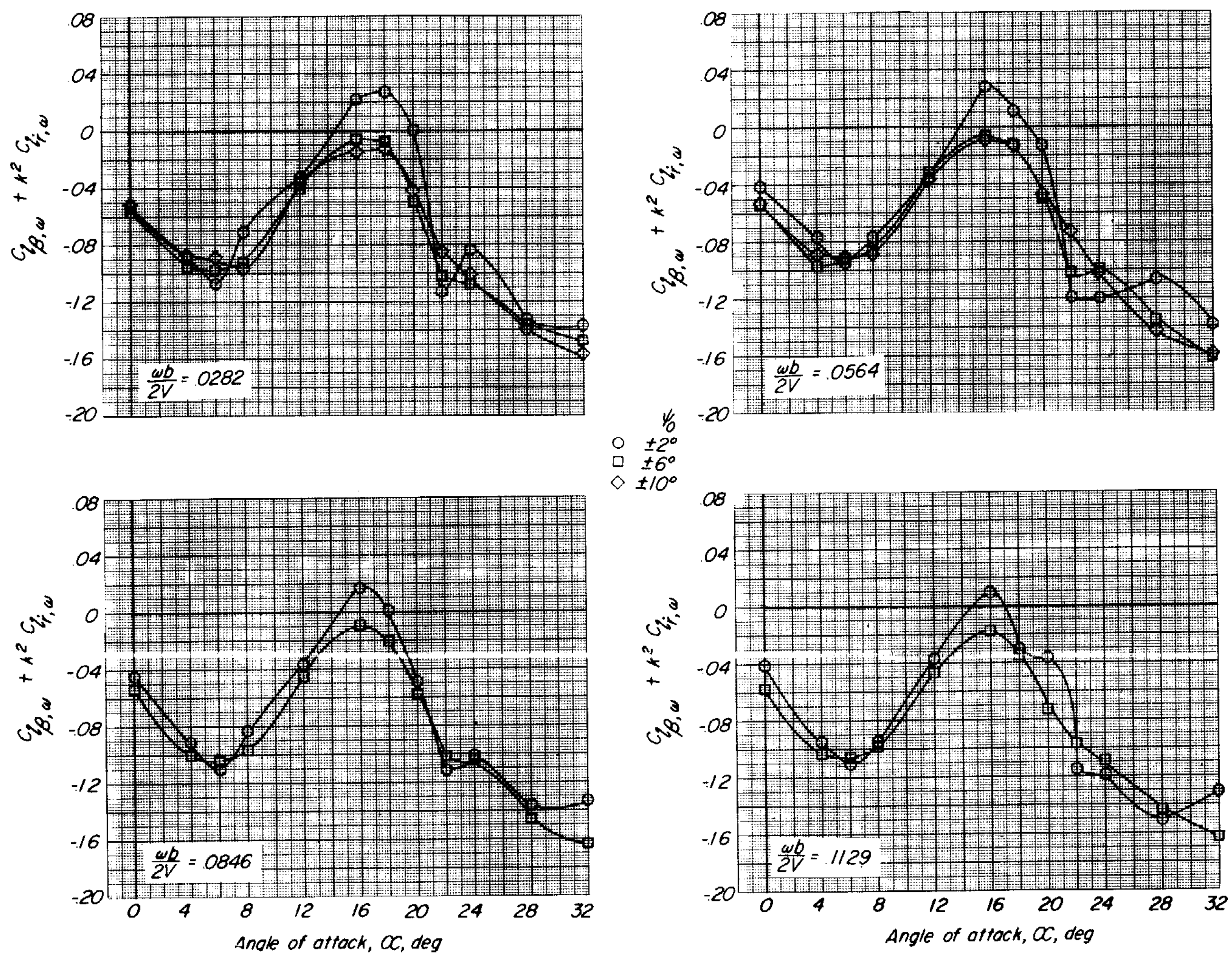

(d) Effective-dihedral characteristics.

Figure 6.- Concluded.

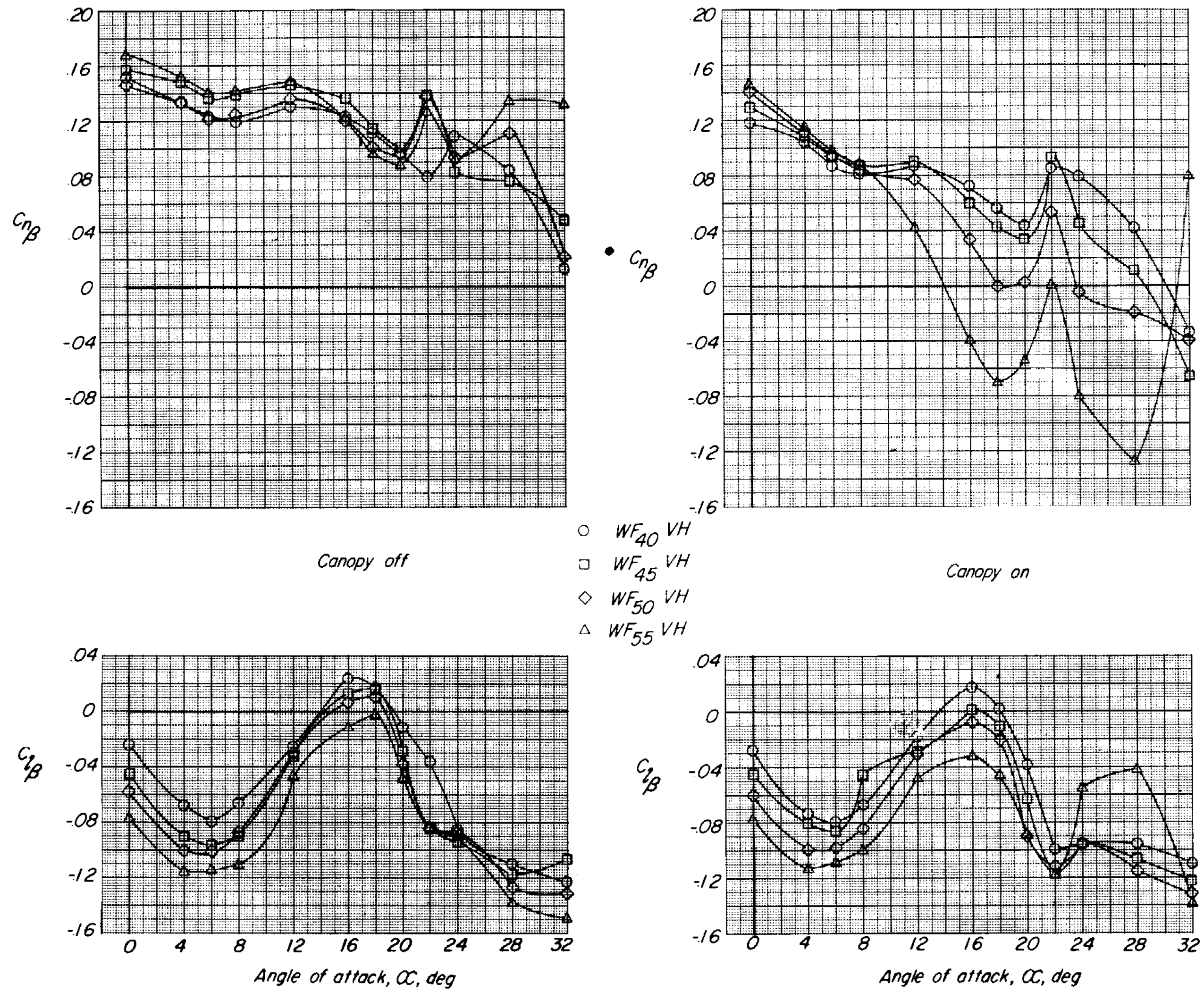

Figure 7.- Effect of fuselage nose length on static-stability derivatives for configurations with canopy on and off.

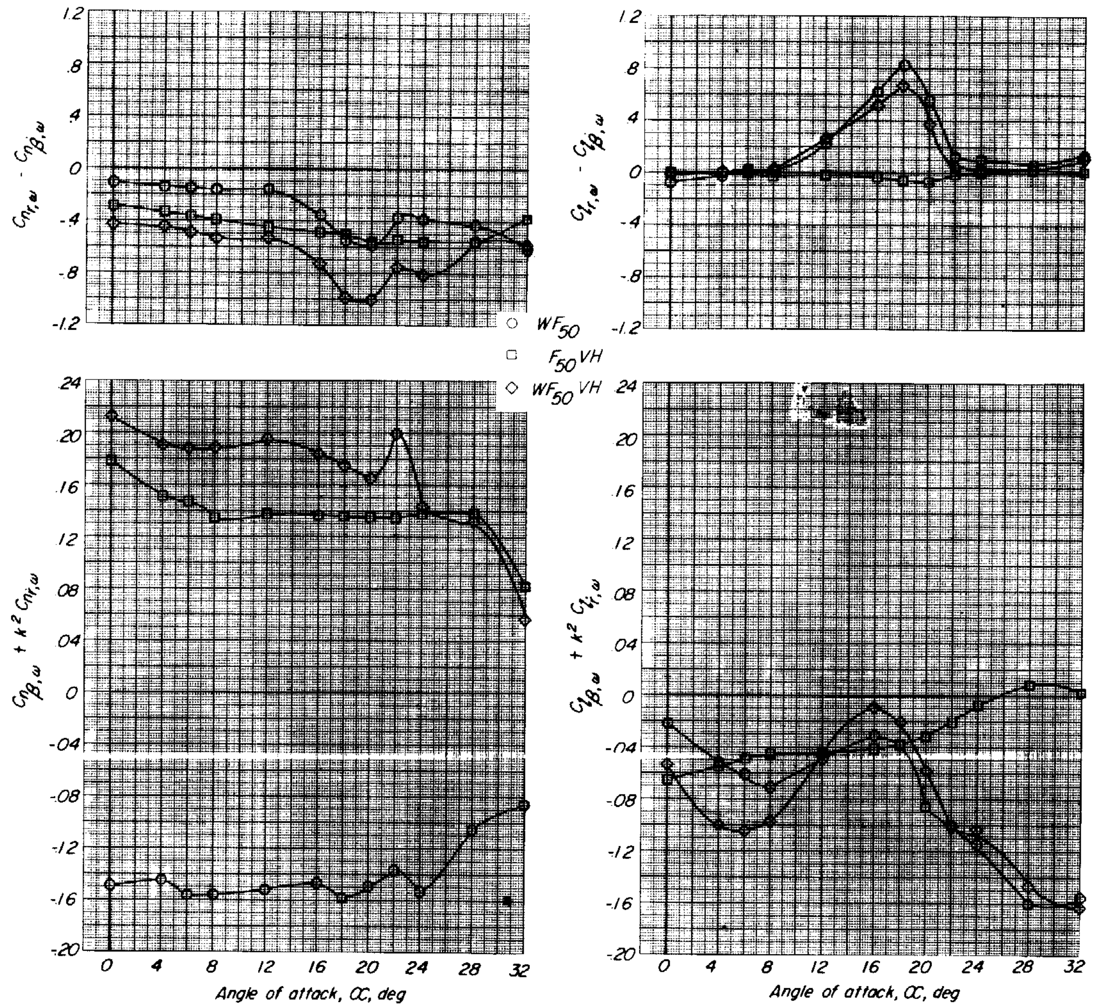

Figure 8.- Stability derivatives measured during oscillation for various model components without canopy. $\frac{\omega b}{2V} = 0.0846$; $\psi_o = \pm 6^o$.

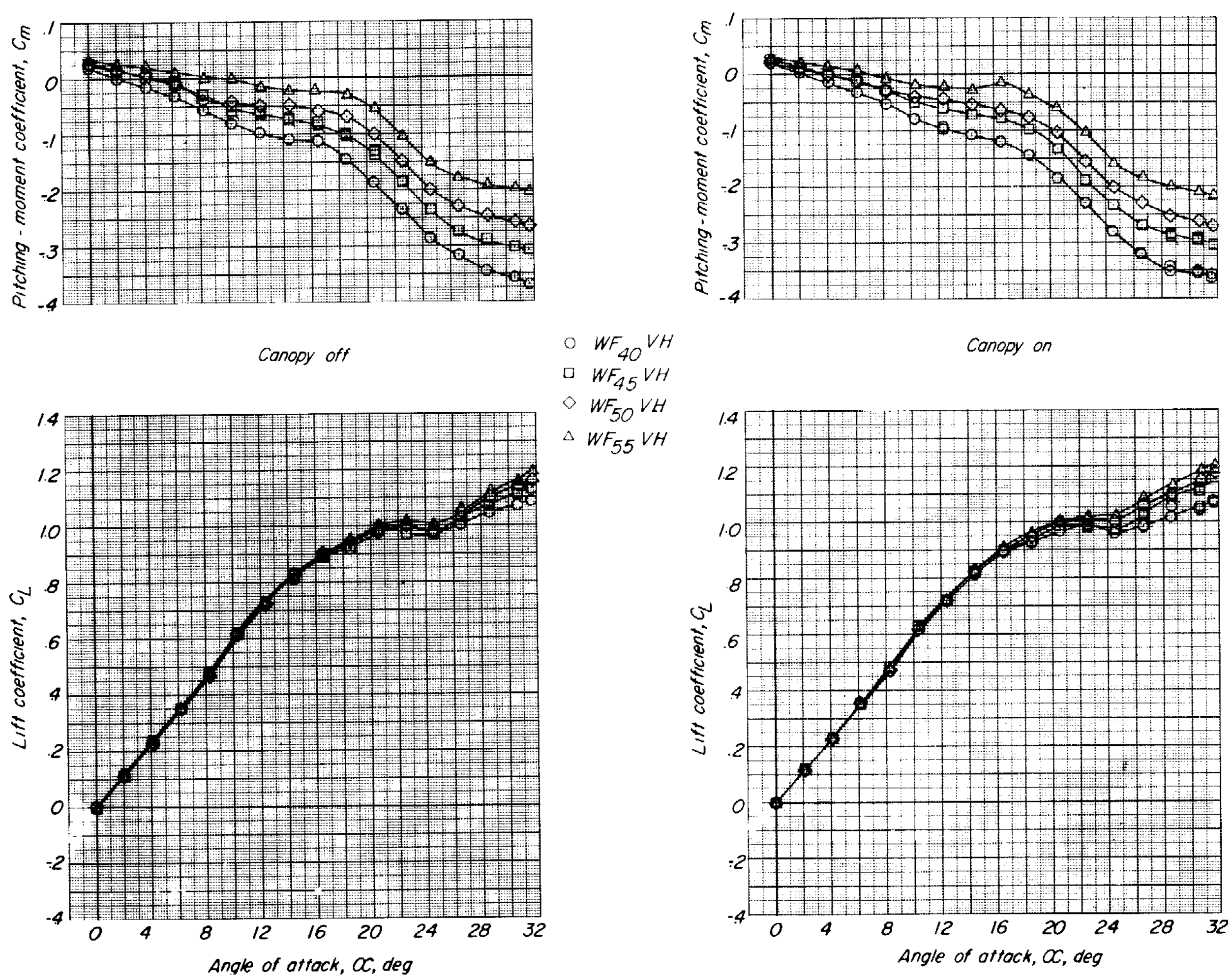

(a) Lift and pitching-moment characteristics.

Figure 9.- Effect of fuselage nose length on lift, approximate drag, and pitching-moment coefficients for configurations with canopy on and off.

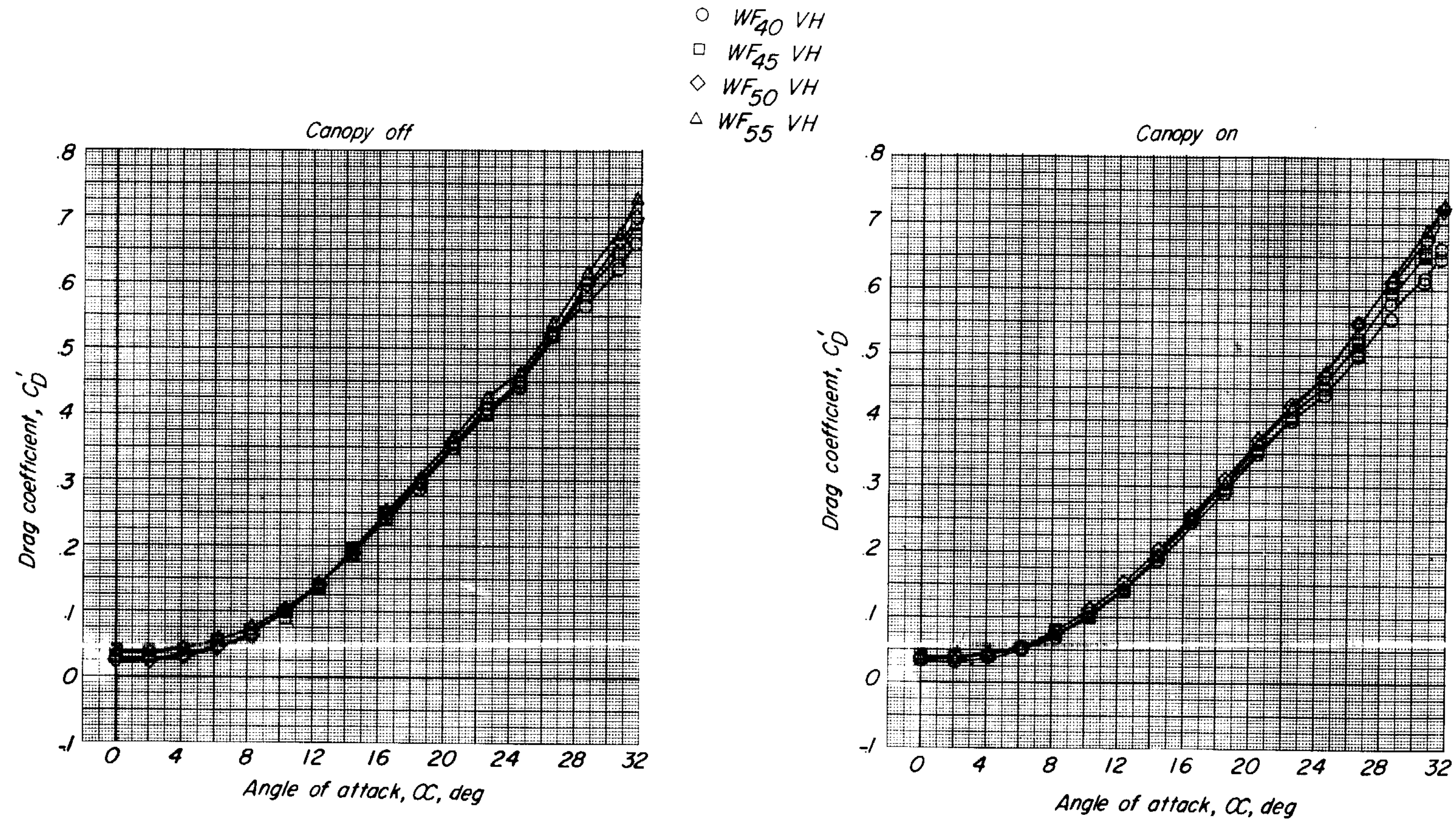

(b) Approximate drag characteristics.

Figure 9.- Concluded.